ISSN 0027-1349, Moscow University Physics Bulletin, 2016, Vol. 71, No. 5, pp. 520–525. © Allerton Press, Inc., 2016.
Original Russian Text © G.N. Nurislamova, M.A. Nosov, 2016, published in Vestnik Moskovskogo Universiteta, Seriya 3: Fizika, Astronomiya, 2016, No. 5, pp. 50–55.

PHYSICS OF EARTH, ATMOSPHERE, AND HYDROSPHERE

The Horizontal Motion of a Water Layer during the Passage of Tsunami Waves Based on Data from a Dense Ocean-Floor Network of Deepwater Sea-Level Stations

G. N. Nurislamova* and M. A. Nosov**

Department of Physics, Moscow State University, Moscow, 119991 Russia
*e-mail: *gulnaz 1205@yandex.ru, **nosov@phys.msu.ru*

Received May 23, 2016; in final form, July 1, 2016

Abstract—A method for the retrieval the horizontal motion of a water layer during the passage of a tsunami wave is proposed based on the data from a dense network of sea-level deepwater stations. The method is applied for calculation of the horizontal velocity of the flow and displacement of water particles in the vicinity of the DONET/JAMSTEC observatories during the passage the 2011 Tohoku tsunami. It was found that the amplitude of the flow speed was ~0.01 m/s, while the amplitude of the displacement exceeded 10 m.

Keywords: tsunami measurements, bottom cable stations, sea level, long waves, horizontal motion.

DOI: 10.3103/S0027134916050143

INTRODUCTION

Over the last 10 years the methods for studying and forecasting tsunami waves have been strongly developed using deepwater sea-level stations [1, 2]. The principle of the deepwater mareograph work (measuring pressure variations by a sensor installed on the ocean bottom) was suggested in the late 1960s [3]. During long-wave passage, the bottom-pressure variations are proportional to the free sea surface displacement from its equilibrium position in the vertical (according to the hydrostatic law), which makes it possible to easily interpret the observed signal. Along with this, the variations of pressure at the ocean bottom are free of noise, which is a manifestation of short surface (wind) waves.

Among the deepwater tsunami-monitoring systems, the Deep-Ocean Assessment and Reporting of Tsunamis (DART) system has become the best known [4], which includes more than 60 stations installed in the tsunami hazard area of the World Ocean. In most cases, DART stations are situated at a considerable distance from one another: the distance between the stations is usually larger than tsunami wave length. This is the reason that retrieval of the wave field based on the DART data is a sophisticated problem that may not have a single solution.

In 2006–2011, the Dense Oceanfloor Network System for Earthquakes and Tsunamis (DONET/JAMSTEC, Japanese Agency for Marine-Earth Science and Technology) was deployed near the Kii peninsula (the Honshu Island, Japan) [5]. The system included several tens of deepwater stations situated at intervals of 15–20 km from one another. In contrast to the sparse network of DART stations, DONET is a dense network system that makes it possible to distinguish the details of the wave field during tsunami passage.

At the time when the catastrophic earthquake occurred in Japan on March 11, 2011 (2011 Tohoku), ten stations of the DONET system were functioning; all of them registered both seismic and oceanic gravity waves associated with this event [6, 7]. The existence of information about the spatial distribution and temporal variability of the ocean-bottom pressure variations provides a unique opportunity for obtaining the horizontal motion of a water layer during the passage of a tsunami wave.

The interest in the horizontal motion is not accidental. It is related to the potential use of these data for an operational tsunami-forecast system. The issue is that the information on horizontal motion can be acquired without sea-level data: for example, with the use of drifters and a satellite navigation system, high-resolution satellite images, or acoustic Doppler current meters.

Previously, the horizontal motion of the water layer associated with the generation and propagation of a tsunami in the open ocean has been studied almost only in the theoretical sense [8–16]. The work [17] is a rare exception to this rule; using accelerometer data the authors discovered the horizontal (1.33 m) and vertical (0.14 m) motions of an iceberg in the Ross Sea during the passage of the Indonesian tsunami in 2004.

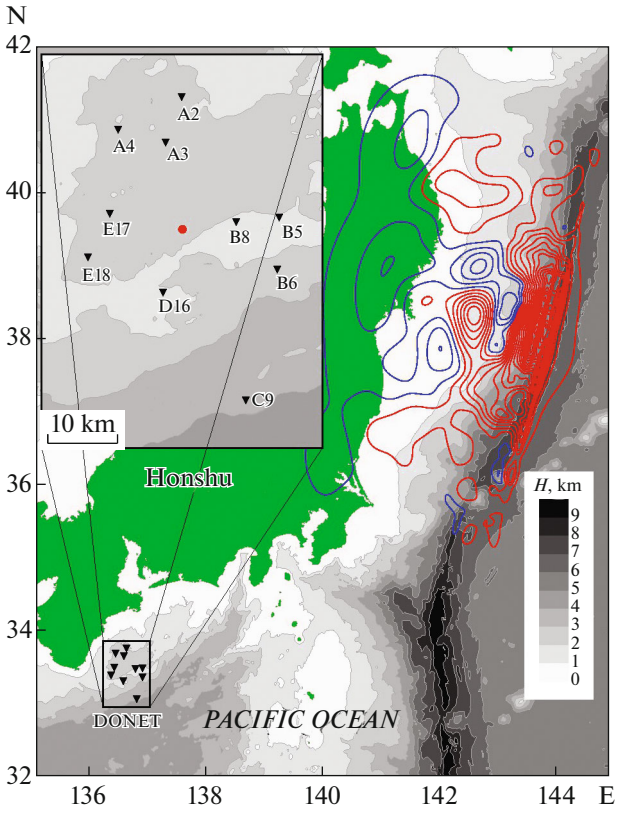

Fig. 1. The relative positions of DONET stations (black triangles) and the origin of the 2011 Tohoku tsunami (significant coseismic deformations of the ocean floor). The red line is uplift; the blue line is subsidence; the step is 0.5 m. Isobaths are drawn at a 1 km interval, the color scale of the depth is in the bottom right corner. DONET station locations are shown in a box in the upper left corner. The length-scale (10 km) is indicated in the bottom part of the box. The red circle shows the point for which the calculations were performed (as shown in Figs. 3 and 4).

The main goals of this work are: (1) the development of a method for obtaining the horizontal motion (velocity and displacement) of the water layer during the passage of a tsunami wave based on the data from deepwater sea-level stations and (2) retrieval of horizontal motion during the 2011 Tohoku tsunami passage based on the data acquired by the DONET system.

To close the Introduction, we note that the developed method for obtaining the horizontal velocity can have direct practical application in tsunami warning systems. Generally speaking, a solution of the forecast problem based on the use of hydrophysical measurements [18] assumes that both the sea-surface displacement data, as well as the horizontal velocity, are introduced in the model. This is due to the fact that the nonlinear equations of the long-wave theory used in prognostic models are written in terms of the free surface displacement and the horizontal velocity.

1. DATA PREPROCESSING

In Fig. 1, the relative positions of the DONET stations and the origin of the 2011 Tohoku tsunami are presented together. The tsunami origin is an area of a significant coseismic deformations of the ocean floor; it is shown with isolines (red lines, uplift; blue lines, subsidence; the step for the isoline is 0.5 m). Coseismic deformations were calculated by the authors of [14] using the Okada formulas [19] with a slip distribution provided by the United States Geological Survey (USGS). The figure shows that the DONET stations were located at a considerable distance from the tsunami origin, viz., approximately 800 km or more.

In Fig. 2, the bottom pressure variations registered by the DONET A2 station are presented as an example (red line). The sampling frequency of signal is equal to 10 Hz. The hydrostatic pressure value (~20 376 kPa) is several orders of magnitude higher than the amplitudes of the variations (~40 kPa); thus, it was preliminarily subtracted from the signal shown in the figure. The variation of the bottom pressure is a superposition of the seismic, hydro-acoustic, and gravity waves. The arrival of seismic waves in the records is seen a few minutes after the start of the main earthquake (Mw 9.0, 05:46:24 UTC) and after the first strong aftershock (Mw 7.9, 06:15:40 UTC). The leading tsunami wave arrived only 1 hour after the main earthquake. It is remarkable that the seismic waves and the hydroacoustic waves generated by them appear with much higher amplitudes in the records compared with the tsunami waves [2, 7].

The method of retrieval of the horizontal motion of the water layer during the passage of a tsunami wave is based on a long-wave theory. The theory applied to the data processing of the measured bottom pressure variations implies that only the components that correspond to long gravity waves should be extracted from the initial data. The signal-processing procedure was as follows.

At the *first stage* the variations of pressure were brought to the zero level by subtraction of the mean over the 4.5-day (from 09:00 March 10, 2011, to 21:00 March 14, 2011) value of the signal. During this period all of the ten stations were performing without interruption. Normalizing a signal to a zero level is necessary to remove the statistical error in bottom-pressure measurements.

At the *second stage* the high frequencies, which are irrelevant for gravity waves, were filtered from the variations of pressure. In fact, for a monochromatic wave the free water-surface displacement relative to the equilibrium position ξ is related to the bottom-pressure variations p by the following classical formula [20]:

$$\frac{p}{\rho g \xi} = \frac{1}{\cosh(kH)}, \qquad (1)$$

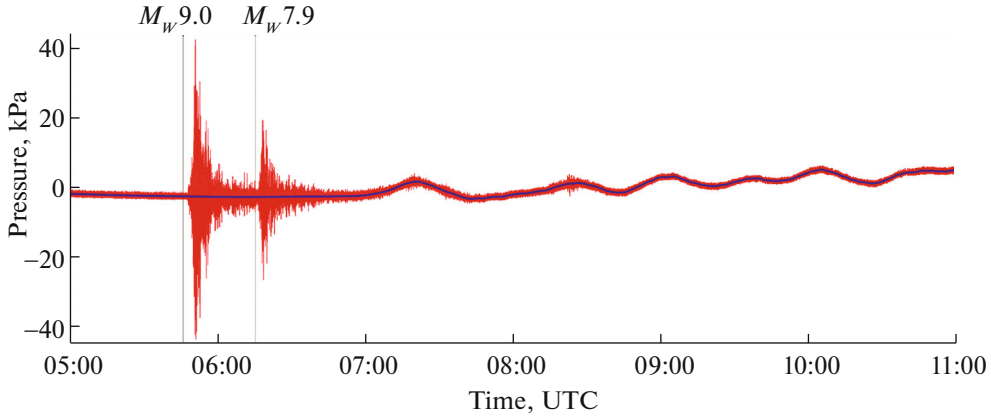

Fig. 2. The ocean-bottom pressure variations registered by the A2 station of the DONET system during the Tohoku earthquake and tsunami in 2011: the red line represents the initial signal; the blue line gives the result of low pass filtering with a cutoff frequency of 0.005 Hz. The data was preliminarily normalized to the zero level by subtraction of the hydrostatic pressure (~ 20 376 kPa). The times of the beginning of the main earthquake (Mw 9.0) and the first strong aftershock (Mw 7.9) are indicated with vertical lines.

where g is gravitational acceleration, H is the ocean depth, ρ is the water density, and k is the wave number, which is linked to the wave's angular frequency by the dispersion relationship $\omega^2 = gk\tanh(kH)$. From the equation (1) it follows that the short (high-frequency) waves occur in the variation of the bottom pressure with attenuation or do not occur at all, while the long waves occur without attenuation following the hydrostatic law $p = \rho g\xi$. This peculiarity is used for the interpretation of gravity waves measured by the bottom-pressure gauges [1, 2, 21]. Thus, when eliminating the high-frequency part of the signal that is irrelevant to the long gravity waves, the cutoff filter frequency f_c was chosen in such a way that the variations of the bottom pressure p were in accordance with the hydrostatic law $p = \rho g\xi$ with an accuracy higher than 10% [12, 18]:

$$f_c \approx 0.0718\sqrt{g/H}. \qquad (2)$$

The stations of the DONET system are installed at depths from 1924 m (B8) to 3511 m (C9); most of them are placed at a depth of approximately 2000 m. The filter cutoff frequency for the depth of 2000 m calculated using equation (2), is equal to f_c~0.005 Hz. For the following data processing, it is important that the minimum wavelengths of the gravity waves ($\lambda_c = \sqrt{gH}/f_c \approx 13.9H \approx 28\,000$ m) are comparable and in some cases exceed the distances between the stations.

The result of the low-pass filtering of pressure variations (the cutoff frequency $f_c \approx 0.005$ Hz) at the A2 station is shown in Fig. 2 with a blue line. The high-frequency components of the signal corresponding to the seismic and acoustic waves are omitted, while the tidal- and tsunami-wave manifestations remain unchanged.

At the *third stage* of the data processing, the sampling frequency of signal was reduced from 10 Hz to 0.1 Hz. After filtration, this procedure could be carried out without a loss of information. Further, for every discrete moment of time, an interpolation function (spline) was constructed based on the pressure values at ten key points whose locations were defined by the geographical coordinates of DONET stations. The function describes the spatial distribution of pressure inside the area of the deployment of the stations.

As a result of the initial data processing, we obtained an analytical assessment in space and discretized assessment in time of the bottom-pressure field $p(Lon,Lat,t_i)$, where Lon is longitude, Lat is latitude, and t_i is the discretized moments of time.

2. RETRIEVING THE HORIZONTAL MOTION: METHODS AND RESULTS

In Fig. 3a, the sea-level dynamics calculated with an interpolation function $p(Lon, Lat, t_i)$ are shown for a point located approximately in the center of the DONET stations (Lat = 33.45° N, Lon = 136.65° E). The location of this point is shown in Fig. 1 as a red circle. We took the free-surface displacement to be related to the bottom pressure via the hydrostatic law $\xi(Lon, Lat, t_i) = p(Lon, Lat, t_i)/\rho g$. The following values of the water density and gravitational acceleration were used for the numerical calculations: ρ = 1030 kg/m^3, g = 9.8 m/s^2.

From Fig. 3a it is clear that both tidal and tsunami waves occur in the sea-level variations. The amplitude of the sea-level variations (~1 m) is substantially smaller than the ocean depth in the area under consideration (H ~ 2000 m), which makes it possible to apply linear long-wave theory [2, 8]. The observed period of tsunami waves (~1 h) is noticeably inferior to the Earth's rotation period. This suggests neglecting the Coriolis and tidal forces in the equations. Taking all of

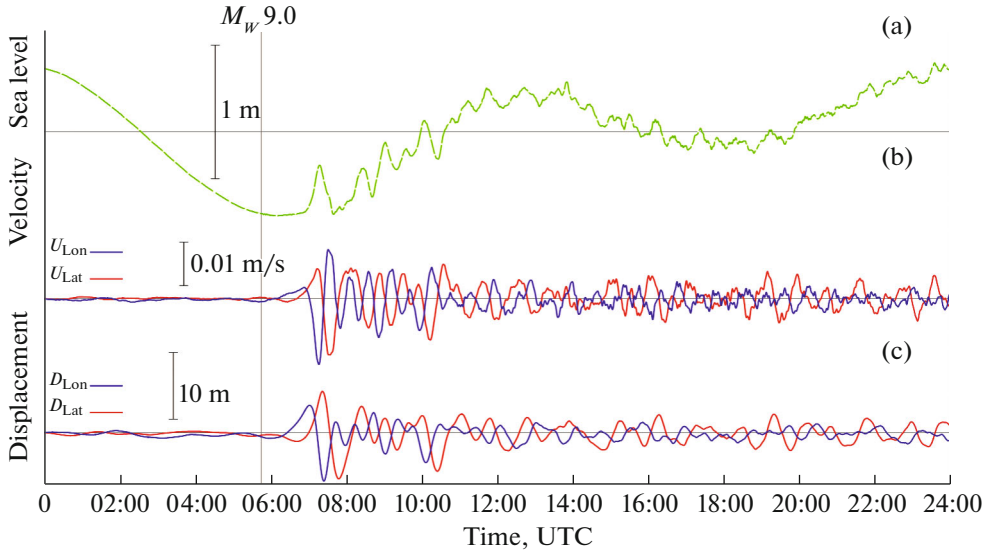

Fig. 3. Sea level (a;) longitudinal and latitudinal components of the horizontal velocity (b); the longitudinal and latitudinal components of the horizontal displacement of water particles (c); during the passage of 2011 Tohoku tsunami waves, reconstructed based on the data from the DONET stations at the point with coordinates *Lat* = 33.45° N, *Lon* = 136.65° E (red circle in Fig. 1). The characteristic scales (1 m, 0.01 m/s, 10 m) are shown with vertical segments. The beginning of the main earthquake (Mw 9.0) is indicated with a vertical line.

these assumptions into account, the dynamic equation of the linear long-wave theory is as simple as:

$$\frac{\partial \mathbf{U}}{\partial t} = -g\nabla\xi, \qquad (3)$$

where $\mathbf{U} = (U_{\text{Lon}}, U_{\text{Lat}})$ is the vector of the horizontal current velocity and it's longitudinal and latitudinal components and ∇ is a differential operator applied in the horizontal plane. The vector $\nabla\xi$ components were calculated with the bottom pressure field $p(Lon, Lat, t_i)$ using the relation $\xi = p/\rho g$.

If the right side of equation (3) is known, the field of the horizontal velocity can be calculated by a direct integration of the equation in time. The initial field of the current velocity is considered to be zero. It should be noted that in fact we are not calculating the velocity itself, but an addition to the existing background ocean currents; the linearity of the problem makes it possible to apply the superposition principle.

The procedure of integration over time in the frequency domain is equivalent to division by the frequency. Therefore, this procedure leads to the intensification of the low-frequency components of the signal. Integration over time of a function that is known approximately (from in situ measurements) usually brings errors that increase in time. To avoid this effect, the time series of vector $\nabla\xi$ components were processed additionally according to the following scheme. A moving average with a Gaussian window was applied to each time series. The averaged time series was then extracted from the initial series. Actually, this type of processing is similar to a low pass filter, which, in any case, brings the initial time series to the zero mean level. The width of the filter window was chosen in such a manner that a signal with a period below 3600 s would be reconstructed without distortion, while longer-period variations would be suppressed. Finally, taking the data preprocessing described in the part 1 into account, we obtained a signal within a range of periods from 200 s to 3600 s, which corresponds to a classical range of tsunami-wave periods [2, 8].

The obtained latitudinal and longitudinal components of the current velocity at the point with the coordinates *Lat* = 33.45° N, *Lon* = 136.65° E (red circle in Fig. 1) on March 11, 2011, from 00:00 to 24:00 UTC are shown in Fig. 3b. The retrieval of the horizontal current velocity for other points within the area of DONET stations gives similar results. Therefore, we will confine ourselves to only one example of calculations for this point. Figure 3b shows that the longitudinal and latitudinal components of velocity have a small amplitude (~0.01 m/s). From the estimates provided in [18] it follows that the time it takes for a long wave to reach the shore from the point under consideration here does not exceed 1000 s. For this reason, only a leading tsunami wave can be regarded as running wave at this point. At the following stages, the wave perturbation is a superposition of the running and reflected waves as well as those trapped on the shelf. For a running sinusoidal long wave, the amplitude of the current velocity and the sea-surface displacement are related by the simple formula [8]:

$$u = \xi\sqrt{g/H}, \qquad (4)$$

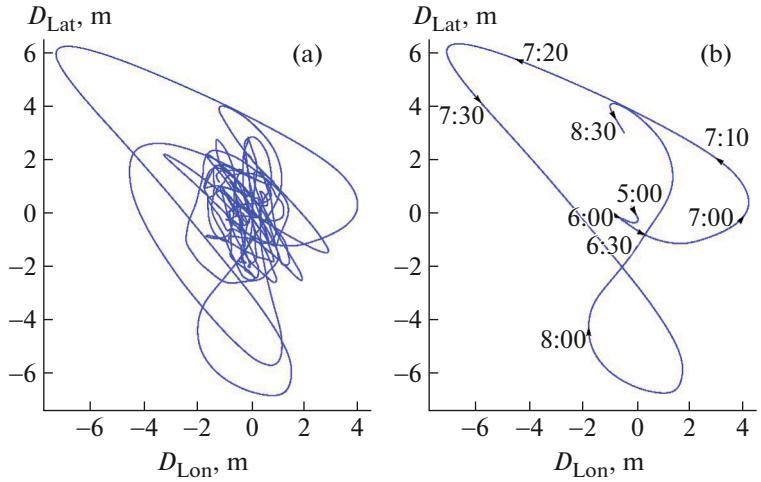

Fig. 4. The horizontal displacement of water particles (track) during the passage of the 2011 Tohoku tsunami waves, reconstructed based on the data from the DONET stations in the point with coordinates *Lat* = 33.45°N, *Lon* = 136.65° E (red circle in Fig. 1): (a) from 00:00 to 24:00 UTC; (b) from 05:00 to 08:40 UTC.

which makes it possible to obtain an independent estimate for the velocity of a leading tsunami wave. From Fig. 3a, it is clear that the amplitude of the leading tsunami wave was $\xi \approx 0.3$ m. The ocean depth at this point (*Lat* = 33.45° N, *Lon* ≈ 136.65° E) is equal to $H \approx$ 2039 m according to GEBCO database. Putting these values into equation (4) one can obtain the estimate $u \approx 0.02$ m/s, which corresponds well to the amplitude of the leading tsunami wave velocity via the integration of equation (3): $\sqrt{U_{Lon}^2 + U_{Lat}^2} \approx 0.017$ m/s.

Finding velocities on the order of a few cm/s among other oceanic processes is a challenging task. Nevertheless, it is worth mentioning that during the passage of a tsunami wave all of the water column is moving in the same way in the horizontal. It may be that use of that particular feature (e.g., a system of drifters situated at different depth) will make it possible to detect weak currents associated with a tsunami in the open ocean.

It is known that when a tsunami wave reaches shallow water, the amplitude of the wave increases following Green's law: $\xi \sim H^{-1/4}$ [2, 8]. Taking Green's law and equation (4) into account one can obtain that with a decrease of depth the amplitude of the horizontal current velocity grows much faster than the amplitude of the waves: $u \sim H^{-3/4}$. A rapid increase of the current velocity in shallow areas, on one hand, provides a more robust method to discover tsunamis, but, from on the other hand, close to the shore these currents can be dangerous for navigation.

Integrating the current speed over time makes it possible to obtain the horizontal displacements of water particles. The procedure of signal processing here was similar to that used for the retrieval of the current speed. In Fig. 3c, the dynamics of the horizontal displacement of water particles (latitudinal and longitudinal components) is presented for March 11, 2011, in the vicinity of a point with coordinates *Lat* = 33.45 N, *Lon* = 136.65°E (red circle in Fig. 1). The corresponding water particle trajectory is provided in Fig. 4. The figure shows clearly that the most intensive motion is correlated with the passage of tsunami leading wave; the motion is then attenuated slowly. In general, the nature of the horizontal motion obtained from the DONET data corresponds well to the results of numerical modeling [14]. The visible randomness and duration of horizontal motions associated with tsunami waves is due to the effect of trapped waves. The amplitude of the horizontal motion of water particles is 10 m, which is more than an order of magnitude higher than the amplitude of vertical motion (sea surface displacement is ~0.3 m). Such noticeable horizontal displacements certainly can be detected by drifters equipped with a satellite navigation system.

CONCLUSIONS

A method of retrieving the horizontal motion of a water layer during the passage of tsunami waves is proposed based on the data from a dense network of deep-water sea-level stations. The method employs direct integration of dynamic equation of a long wave theory with a known right-hand side, which is a pressure gradient force. The latter is calculated by interpolating the sparse point measurements of bottom pressure. A data-processing procedure is described: the initial time series of pressure variations are treated with a low-pass filter as a key stage of the procedure, as low frequencies are associated with long waves.

The efficiency of this method was demonstrated based on the example of the catastrophic tsunami (the 2011 Tohoku) of March 11, 2011. The tsunami was recorded by the DONET/JAMSTEC network of bot-

tom observatories that are deployed at depths of approximately 2000 m, which are located over 800 km away from the tsunami origin. It was found that the amplitude of the horizontal current velocity in tsunami waves was 0.01 m/s and the horizontal displacements (~10 m) were larger by more than an order of magnitude than the sea surface level variations in the vertical plane (~0.3 m).

ACKNOWLEDGMENTS

The DONET data were obtained in the context of the complementary Agreement between the Department of Physics of Moscow State University and the Japanese Agency for Marine-Earth Science and Technology on Early tsunami detection methods on the basis of a real-time seafloor observatory network (2013). We are grateful to JAMSTEC for the provided data. The project was supported by the Russian Foundation for Basic Research, project nos. 16-35-00231, 16-05-00053, and 16-55-50018.

REFERENCES

1. A. B. Rabinovich, Izv., Atmos. Ocean. Phys. **50**, 445 (2014).
2. B. W. Levin and M. A. Nosov, *Physics of Tsunamis*, 2nd ed. (Springer, 2016).
3. S. L. Solov'ev, *Tsunami Problem* (Nauka, Moscow, 1968).
4. E. Bernard and C. Meinig, in *Proc. OCEANS Conf., Kona, 2011* (IEEE, 2011). http://www.pmel.noaa.gov/pubs/PDF/bern3802/bern3802.pdf.
5. Y. Kaneda, in *Proc. OCEANS Conf., Seattle, 2010* (IEEE, 2010). doi 10.1109/OCEANS.2010.5664309
6. H. Matsumoto and Y. Kaneda, in *Proc. XI SEGJ Int. Symp., Yokohama, 2013*, p. 493.
7. M. A. Nosov, K. A. Sementsov, S. V. Kolesov, H. Matsumoto, and B. W. Levin, Dokl. Earth Sci. **461**, 408 (2015).
8. E. N. Pelinovskii, *Tsunami Wave Hydrodynamics* (Inst. Prikl. Fiz., Novgorod, 1996).
9. L. Kh. Ingel', Dokl. Earth Sci. **362**, 1036 (1998).
10. S. F. Dotsenko, Izv., Atmos. Ocean. Phys. **35**, 641 (1999).
11. S. F. Dotsenko and Yu. I. Shokin, Vychisl. Tekhnol. **6**, 13 (2001).
12. M. A. Nosov, A. V. Moshenceva, and B. W. Levin, Dokl. Earth Sci **438**, 853 (2011).
13. M. A. Nosov and G. Nurislamova, Moscow Univ. Phys. Bull. **67**, 457 (2012).
14. M. A. Nosov, A. V. Moshenceva, and S. V. Kolesov, Pure Appl. Geophys. **170**, 1647 (2013). doi doi 10.1007/s00024-012-0605-2
15. M. A. Nosov and G. Nurislamova, Moscow Univ. Phys. Bull. **68**, 490 (2013).
16. M. A. Nosov, G. N. Nurislamova, A. V. Moshenceva, and S. V. Kolesov, Izv., Atmos. Ocean. Phys. **50**, 520 (2014).
17. E. A. Okal and D. R. MacAyeal, Seismol. Res. Lett. **77**, 659 (2006).
18. M. A. Nosov and S. S. Grigorieva, Moscow. Univ. Phys. Bull. **70**, 326 (2015).
19. Y. Okada, Bull. Seismol. Soc. Am. **75**, 1135 (1985).
20. H. Lacombe, *Cours d'océanographie physique (Théories de la circulation générale. Houles et vagues)* (Gauthier-Villars, Paris, 1965).
21. K. I. Kuznetsov, A. A. Kurkin, E. N. Pelinovksy, and P. D. Kovalev, Izv., Atmos. Ocean. Phys. **50**, 213 (2014).

Translated by A.D. Tarasenko